Article

Constraining Dense Matter Physics Using f-Mode Oscillations in Neutron Stars

Sukrit Jaiswal [1] and Debarati Chatterjee [2,*]

[1] Indian Institute of Science Education and Research, Dr. Homi Bhabha Road, Pashan, Pune 411008, India; sukrit.jaiswal@students.iiserpune.ac.in

[2] Inter-University Centre for Astronomy and Astrophysics, Pune University Campus, Pune 411007, India

* Correspondence: debarati@iucaa.in

Abstract: In this paper, an investigation of the role of nuclear saturation parameters on f-mode oscillations in neutron stars is performed within the Cowling approximation. It is found that the uncertainty in the effective nucleon mass plays a dominant role in controlling the f-mode frequencies. The effect of the uncertainties in saturation parameters on previously-proposed empirical relations of the frequencies with astrophysical observables relevant for asteroseismology are also investigated. These results can serve as an important tool for constraining the nuclear parameter space and understand the behaviour of dense nuclear matter from the future detection of f-modes.

Keywords: neutron stars; gravitational waves; f-modes; dense matter

1. Introduction

With the direct detection of gravitational waves (GWs) from a binary merger GW170817 of neutron stars (NSs) [1], a new window of opportunity has opened up to directly probe their interior composition. In conjunction with astrophysical observations using multi-wavelength space-based and ground-based telescopes, gravitational wave detectors now introduce the possibility of multi-messenger astronomy, from which several astrophysical NS observables can be derived [2].

Neutron stars are compact remnants of the evolution of massive stars, associated with core-collapse supernovae. These objects have extreme densities up to several times normal nuclear matter density in the core, orders of magnitude beyond matter densities possible to investigate with terrestrial experiments. It is therefore inevitable to resort to theoretical models, in order to extrapolate the known physics at nuclear saturation to higher densities and isospin asymmetries. This extrapolation leads to large uncertainties, reflected by the proliferation of models. Different schemes (ab-initio, phenomenological) have been applied to describe such equations of state (EoS) [3]. The ab initio many-body models use realistic nucleon–nucleon (NN) interaction which is obtained by fitting the NN scattering data. The phenomenological models are based on nuclear density functional theories with effective nucleon-nucleon interactions, which are calibrated by reproducing the nuclear bulk properties around saturation density. Different models show different high-density behavior, resulting in different predictions for NS observables, thus making it difficult to interpret and compare directly with astrophysical data.

NSs are visible throughout the electromagnetic spectrum. A number of global properties of NSs, such as their mass and radius, can be deduced from multi-wavelength astronomical data. Accurate estimations of NS masses using post-Newtonian effects in relativistic NS binaries indicate maximum masses to be close to $2M_{Sun}$ [4,5]. Radius estimates obtained from X-ray data [6] are less precise, but the recently launched NICER mission [7] is soon expected to measure radii with a precision of up to 5%. These observables can be obtained from the NS EoS by solving equations for hydrostatic equilibrium. Comparison

with astrophysical data then allows us to put important constraints on the EoS models and consequently on the nature of dense matter.

GWs are considered one of the most promising tools for constraining dense matter physics, as they can directly probe the interior composition of neutron stars. Quasi-normal modes may be excited in oscillating NSs, producing copious amounts of GWs. These modes, such as fundamental modes (f-modes), pressure modes (p-modes), buoyancy g-modes, rotational r-modes, are classified according to the restoring forces that bring the system back to equilibrium. The most exciting fact is that the mode frequencies and damping timescales contain signatures of the interior composition of neutron stars.

GWs may be emitted from NSs, both isolated or in binary. It was shown that during a merger, the NSs in binary exert strong tidal forces on one another, and the resulting deformation depends on their compactness [1]. This can lead to important constraints on stellar radii and consequently on the dense matter EoS [8]. Further, quasi-normal modes may also be excited during the merger and post-merger phases [9]. In the post-merger phase, if a prompt collapse to a black hole does not occur, the remnant may be a strongly-oscillating NS, as indicated by recent hydrodynamical simulations [10–12]. It is expected that the fundamental quadrupolar fluid mode of the remnant may be strongly excited and may dominate the post-merger GW signal, through generous amounts of gravitational radiation through the Chandrasekhar–Friedman–Schutz (CFS) mechanism when unstable [13].

It is therefore of great interest to constrain the NS EoS using studies of f-modes. The goal of NS asteroseismology is to express the f-mode frequency or damping timescale in terms of global NS observables, independent of the underlying EoS. The goal of NS asteroseismology is to extract the information about its interior and/or that of its global properties from the frequencies. Detection of f-modes would then allow us to invert such relations and obtain constraints for the NS EoS [14–16]. Most of such studies adopted polytropic or parametrized EoSs due to their simplicity [14,17,18]. There are a few investigations that considered realistic equations of state, but only a few representative parameter sets were considered [15,16,19]. Fits using such EoSs have been used to derive relations between mode frequencies and global variables (mean density, compactness). Recently, in [20], the frequency and the damping time of f-modes have been constrained within narrow windows using quite model-independent EOSs derived from the nuclear matter at low densities and perturbative quantum chromodynamcs (QCD) at high densities, connected by interpolating subluminal monotropes at intermediate densities. Although the dispersion of frequencies due to different EoSs in such studies is evident, one cannot compare between the chosen EoSs as they correspond to very different nuclear matter properties. Therefore, it is very difficult to extract any direct information about the role of the underlying nuclear parameters from such studies.

In this paper, the influence of underlying nuclear saturation parameters on f-mode frequencies using Cowling approximation (neglecting background metric perturbations) is investigated. Within the framework of the relativistic mean field (RMF) model, we systematically explore the parameter space allowed by current nuclear experimental data and perform a sensitivity study of the mode frequencies to the uncertainties in each of these parameters. It is also investigated how these uncertainties affect previously proposed empirical relations in the literature, relevant for asteroseismology of non-rotating NSs.

Section 2 describes the microscopic calculation of the EoS as well as the determination of macroscopic NS observables from such an EoS. We also elaborate on the pulsation equations to be solved to obtain f-mode frequencies in non-rotating NSs. The results of our investigations are presented in Section 3, including the sensitivity study and asteroseismology relations. The findings are summarized in Section 4.

It is worth mentioning here that the use of the Cowling approximation in solving the mode frequencies introduces uncertainties (typically 10–30%) exceeding those of the semi-empirical relations sought. However, this is known from previous studies, and the investigation nevertheless gives us a good qualitative idea about how much the uncertainty

in the nuclear saturation parameters affects these relations. This is discussed in detail in Section 2.3.

2. Formalism

2.1. Microscopic Description

As already mentioned in Section 1, this investigation is performed within the framework of the RMF model [21]. Such models have already been applied successfully to describe nuclear matter and nuclei [3]. In order to obtain the EoS of nuclear matter in the RMF Model, let us start with the following interaction Lagrangian density:

$$
\begin{aligned}
\mathcal{L}_{\text{int}} =\ & \sum_N \overline{\Psi}_N \left[g_\sigma \sigma - g_\omega \gamma^\mu \omega_\mu - \frac{g_\rho}{2} \gamma^\mu \vec{\tau} \vec{\rho}_\mu \right] \Psi_N \\
& - \frac{1}{3} bm (g_\sigma \sigma)^3 - \frac{1}{4} c (g_\sigma \sigma)^4 \\
& + \Lambda_\omega (g_\rho^2 \vec{\rho}_\mu \vec{\rho}^\mu)(g_\omega^2 \omega_\mu \omega^\mu) + \frac{\zeta}{4!} (g_\omega^2 \omega_\mu \omega^\mu)^2 ,
\end{aligned}
\tag{1}
$$

where Ψ_N is the Dirac spinor for nucleons N (neutron or proton) and $\overline{\Psi}_N$ is its Dirac adjoint. Further, m is the vacuum nucleon mass, $\gamma^\mu = \{\gamma^0, \gamma^1, \gamma^2, \gamma^3\}$ are the Gamma matrices and $\vec{\tau}$ indicate Pauli matrices. The interaction among the nucleons is mediated by the exchange of the scalar (σ), vector (ω) and the isovector (ρ) mesons. The isoscalar nucleon–nucleon couplings g_σ and g_ω are determined by fixing them to nuclear saturation properties. The σ meson self-interaction terms b and c ensure the correct description of nuclear matter at saturation density. The effective nucleon mass is then defined as $m^* = m - g_\sigma \sigma$. The isovector and mixed ω-ρ couplings g_ρ and Λ_ω can be related to empirical quantities such as symmetry energy, J_{sym}, and its slope, L_{sym} [22–25]. The quartic ω self-coupling ζ is set to zero. The terms $\mathcal{O}(3)$ and higher are not considered here in the expansion with density and asymmetry, as soon as the nuclear experimental data to constrain such parameters have large uncertainties.

The uncertainty in the nuclear empirical quantities derived from state-of-the-art experimental data (saturation density, n_{sat}, energy per particle at saturation, E_{sat}, compressibility, K_{sat}, effective nucleon mass m^*/m, symmetry energy, J_{sym}, and slope of symmetry energy, L_{sym}, is also reflected in the uncertainty in the determination of the RMF model parameters. In order to test the results of this study, first, the two commonly used parametrizations [26], GM1 and GM3, are considered, for which the EoSs are well known. Once the numerical scheme is verified, the entire RMF parameter space, defined by present uncertainties of theoretical and experimental nuclear saturation data, is explored. The range of values of empirical parameters explored in this paper is summarized in Table 1. For each individual parameter "variation", within the ranges shown in Table 1, the others are kept at the "fixed" values.

Given the Lagrangian density Equation (1), one can solve the equations of motion of the constituent particles as well as those of the mesons. In the mean-field approach, the meson fields are replaced by their mean-field expectation values, i.e., $\bar{\omega} = \langle \omega^0 \rangle$, $\bar{\rho} = \langle \rho_3^0 \rangle$. One can then calculate the EoS (pressure-energy density relationship) using this RMF model. The energy density is given by [25]:

$$
\begin{aligned}
\varepsilon =\ & \sum_N \frac{1}{8\pi^2} \left[k_{F_N} E_{F_N}^3 + k_{F_N}^3 E_{F_N} - m^{*4} \ln \frac{k_{F_N} + E_{F_N}}{m^*} \right] \\
& + \frac{1}{2} m_\sigma^2 \bar{\sigma}^2 + \frac{1}{2} m_\omega^2 \bar{\omega}^2 + \frac{1}{2} m_\rho^2 \bar{\rho}^2 \\
& + \frac{1}{3} bm (g_\sigma \sigma)^3 - \frac{1}{4} c (g_\sigma \sigma)^4 \\
& + 3\Lambda_\omega (g_\rho g_\omega \bar{\rho} \bar{\omega})^2 + \frac{\zeta}{8} (g_\omega \bar{\omega})^4 ,
\end{aligned}
\tag{2}
$$

where k_{F_N} and E_{F_N} are the Fermi momentum and energy of the corresponding nucleon N respectively.

The pressure p can be derived from the energy density using the Gibbs–Duhem relation [27],

$$p = \sum_N \mu_N n_N - \varepsilon, \tag{3}$$

where the nucleon chemical potentials are given by

$$\mu_N = E_{F_N} + g_\omega \bar{\omega} + \frac{g_\rho}{2} \tau_{3N} \bar{\rho}. \tag{4}$$

Table 1. Empirical parameter values for RMF models considered in this paper; see text for more details.

Model	n_{sat} [fm^{-3}]	E_{sat} [MeV]	K_{sat} [MeV]	J_{sym} [MeV]	L_{sym} [MeV]	m^*/m
GM1	0.153	-16.3	300	32.5	93.7	0.70
GM3	0.153	-16.3	240	32.5	89.7	0.78
RMF fixed	0.16	-16.0	240	32	60	0.60
variation	[0.15, 0.16]	$[-16.5, -15.5]$	[240, 280]	[30, 32]	[50, 60]	[0.55, 0.75]

2.2. Macroscopic Description

Using the spherical coordinates (t, r, θ, ϕ) for time and space, where θ and ϕ represent spherical angular coordinates, the background spacetime is characterized by a line element,

$$ds^2 = -e^{2\Phi(r)}dt^2 + e^{2\Lambda(r)}dr^2 + r^2 d\theta^2 + r^2 \sin(\theta)d\phi^2, \tag{5}$$

where Φ, Λ are metric functions with respect to r. Given an EoS, the equilibrium configurations of non-rotating relativistic NSs can be obtained by solving the Tolman-Oppenheimer-Volkoff (TOV) equations of hydrostatic equilibrium [27],

$$\begin{aligned} \frac{dm(r)}{dr} &= 4\pi\varepsilon(r)r^2, \\ \frac{dp(r)}{dr} &= -\frac{[p(r) + \varepsilon(r)][m(r) + 4\pi r^3 p(r)]}{r(r - 2m(r))}, \\ \frac{d\Phi(r)}{dr} &= -\frac{1}{(\varepsilon + p)}\frac{dp}{dr}. \end{aligned} \tag{6}$$

Integrating the TOV equations from the center of the star to the surface, one can obtain global NS observables, such as mass, M, radius, R, and compactness, $C = M/R$. The boundary conditions that must be satisfied are a vanishing mass, $m|_{r=0} = 0$, at the centre of the star, and a vanishing pressure, $p|_{r=R} = 0$), at the surface, along with the metric function, $\Phi|_{r=R} = \frac{1}{2}\ln(1 - 2M/R)$, at the surface of the star. The tidal deformability, Λ, can be obtained by solving a set of differential equations coupled with the TOV equations [28]. These can then be compared to the state-of-the-art limits, derived from astrophysical data, in order to impose constraints on the dense matter EoS.

All the EoS curves—pressure p vs. energy density ε—considered in this paper are displayed in Figure 1. Each curve corresponds to a different empirical parameter set from Table 1. The total mass, M (in solar mass M_{Sun}) and radius, R, corresponding to each EoS curve from Figure 1, are given in Figure 2. It is evident from Figure 2 that for all the EoSs, considered here, the maximum masses lie above $2M_{Sun}$ indicated by a horizontal dotted line in Figure 2.
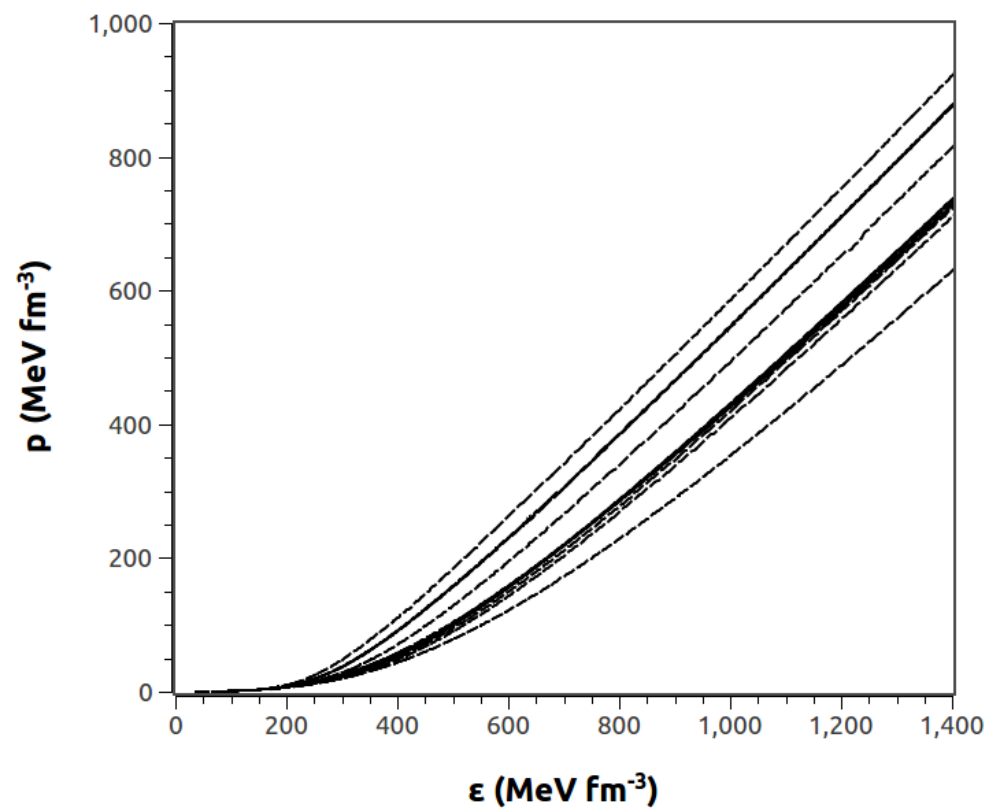
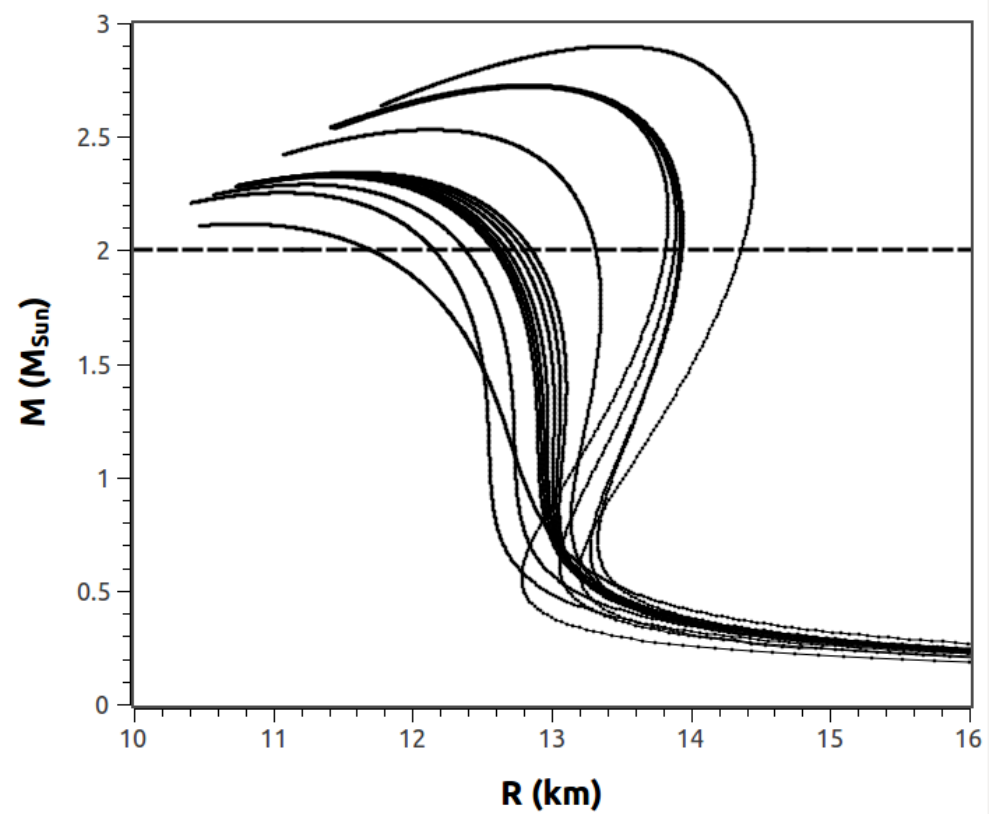**Figure 1.** Equations of state used in this paper; see text for details.

Figure 2. Mass–radius relations corresponding to the equations of state plotted in Figure 1.

In this study, we have not imposed observational constraints on radii. The reason is that the precise determination of NS radii is an ongoing effort and the radius constraints (from X-ray binary data and thermonuclear bursts [6], GW [8] and NICER [7] data) are model-dependent and less robust than those of the maximum mass. The recent analysis [8] of tidal deformabilities from GW170817 led to the determination of the statistically most probable radius of 1.4 M_{Sun} NS. A detailed discussion in [25] narrates how this most probable value for radius changes depending on the models used [8,29–31]. It was also shown that imposing this constraint would disfavor values of effective mass $m^*/m < 0.6$, and this would also apply to the investigation in this paper.

2.3. Solving the Mode Pulsation Equations

The aim of this study is to investigate the influence of the uncertainty in the empirical nuclear parameters on NS f-modes. In general, one must solve coupled fluid and space-time perturbation equations to obtain the mode frequencies [32–39]. However, the situation simplifies if one considers weak gravitational fields and neglect the metric perturbations. This approach, known as the Cowling approximation (CA) [40], has been widely applied for studying Newtonian as well as relativistic NSs.

Although, ideally, one must employ fully linearized equations in general relativity, it has been shown that the difference on applying the CA is less than 20% for f-modes [41]. The differences between frequencies obtained from the CA and the ones obtained from the full set of linearized equations have already been studied in the literature. e.g., in Figure 8 of [42] and Figure 5 of [43] the two calculations have been compared, and it has been demonstrated that the error due to CA is in the range ∼15–30% for f-modes and ∼10% for g-modes, which is fairly decent given the drastic simplification of the calculations. These studies show that the CA tends to underestimate the frequency of the f-mode and that the error of the CA for the f-mode tends to decrease as the mass of the star gets larger [42].

Here, only non-rotating NSs are considered; see Ref. [19] for investigations of f-modes in rotating NSs. The fluid Lagrangian displacement vector is defined by

$$\xi^i = (e^{-\Lambda}W, -V\partial_\theta, -V\sin^{-2}\theta\partial_\phi)r^{-2}Y_{lm}(\theta, \phi), \tag{7}$$

where i is the vector index and $\partial_\theta = \partial/\partial_\theta$ etc., $W(t, r)$ and $V(t, r)$ are functions of r and t. The fluid perturbations are decomposed into spherical harmonics $Y_{lm}(\theta, \phi)$ of degree $l = 0, 1, 2, \ldots$ and order $m = -l, \ldots, l$. Using these variables, the perturbation equations for the fluid oscillations can be obtained from the conservation of the energy–momentum tensor $\delta(\nabla_\nu T^{\mu\nu}) = 0$. For a harmonic time dependence, the perturbation functions can be written as $W(t, r) = W(r)e^{i\omega t}$ and $V(t, r) = V(r)e^{i\omega t}$. On simplification, the pulsation equations required to be solved in order to obtain these frequencies are given by [39]:

$$\begin{aligned}
\frac{dW(r)}{dr} &= \frac{d\epsilon}{dp}\left[\omega^2 r^2 e^{\Lambda(r)-2\Phi(r)}V(r) + \frac{d\Phi(r)}{dr}W(r)\right] - l(l+1)e^{\Lambda(r)}V(r), \\
\frac{dV(r)}{dr} &= 2\frac{d\Phi(r)}{dr}V(r) - \frac{1}{r^2}e^{\Lambda(r)}W(r).
\end{aligned} \tag{8}$$

The functions $V(r)$ and $W(r)$, along with the frequency ω, characterize the perturbation vector. We solve the coupled Equation (8) on a fixed background metric from the origin ($r = 0$), where the solutions behave approximately like [41,44]

$$V(r) = \frac{C}{l}r^l,$$

$$W(r) = Cr^{l+1},$$

where C is an arbitrary constant. The other boundary condition that needs to be fulfilled is that the Lagrangian perturbation to the pressure must vanish at the star's surface, $r = R$. Such condition reads:

$$\omega^2 e^{\Lambda(R)-2\Phi(R)} V(R) + \frac{1}{R^2}\left(\frac{d\Phi}{dr}\right)\bigg|_{r=R} W(R) = 0. \tag{9}$$

In full general relativity (no Cowling approximation), the solution to the perturbation equations are complex, whose real part corresponds to mode frequencies and imaginary part to the damping time. However, in the Cowling approximation, the solutions yield only real mode frequencies ω.

3. Results

3.1. Testing the Numerical Scheme

In order to test the numerical scheme, first, the well-known results for f-mode frequencies for the GM1 parameter set (see e.g., [41,44]) and also for the GM3 set are reproduced. In Figure 3 one displays the fundamental f-mode frequencies, $\nu = \omega/2\pi$, where ω is the solution to perturbation equations, as a function of total mass M (in M_{Sun}) for these two reference parameter sets. As expected, the f-modes have frequencies within 1–3 kHz compatible with previous results reported in literature [41,44].
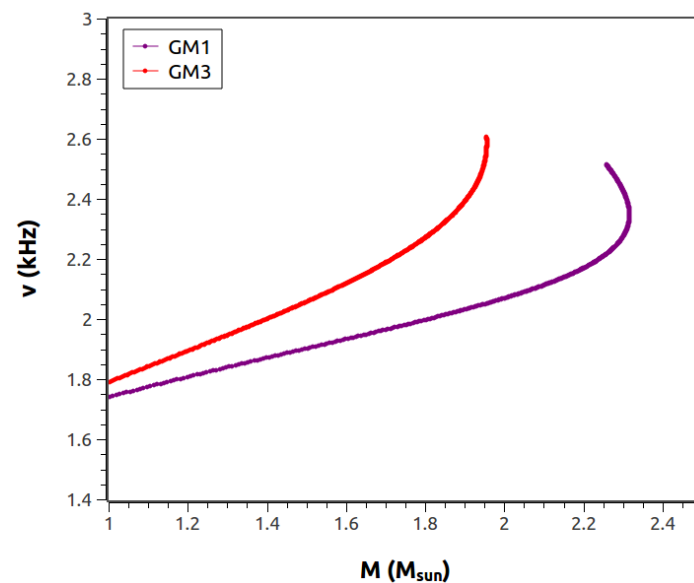

Figure 3. The f-mode frequencies, ν, as a function of total mass. M, for the parameter sets GM1 and GM3.

It must be noted here that the f-mode frequencies for low mass stars will change when one considers interactions with other modes (such as p-modes or g-modes) due to avoided crossings [45]. For this reason, we confine the results of this study to NS masses above 1 M_{Sun} To note here is that the typical f-mode frequency from low-mass neutron stars is $\sim$kHz, which is not in the sensitivity range of the current gravitational wave detectors. There is a possibility that the next generation of detectors, such as the Einstein telescope, will be able to probe f-mode frequencies from low-mass NSs.

3.2. Sensitivity Study

3.2.1. Calculation of $l = 2$ f-Modes

In Section 2, the uncertainties associated with the nuclear saturation parameters, which in turn result in the uncertainty in the EoS, were discussed. Having tested the numerical scheme of the f-mode frequencies in Section 3.1, the study is extended here to investigate the entire parameter space. Each of the nuclear saturation parameters are varied one by one

within their known uncertainties listed in Table 1 and study the sensitivity of the f-mode frequencies to each of the variations.

Variations of the RMF parameters m^*/m, J_{sym} and L_{sym} were performed in [25] within the ranges compatible with the estimations from a variety of experimental, observational and theoretical calculations. Similarly, in the present study, these saturation nuclear parameters were varied along with the other parameters ρ_{sat}, E_{sat} and K_{sat}, within the parameter space (see Table 1) compatible with current uncertainties in experimental data. Parameter sets such as GM1 or GM3 are points that lie within this allowed parameter space. As these EoS parametrizations like GM1, GM3 are obtained by fitting the couplings to reproduce certain chosen experimental data, the influence of any individual saturation parameter on the f-mode frequencies is not clear from a comparison of such EoSs. For example, let us consider the sets GM1 and GM3: one cannot compare the f-mode frequencies for these two sets because the sets differ both in K_{sat} and m^*/m, while the other parameters are the same. So, in order to extract the influence of each individual saturation parameter on f-mode frequencies, one must perform a sensitivity study by varying them one by one within the present experimental uncertainties, keeping the others fixed, as it is done here.

In Figure 4, f-mode frequencies, ν, are displayed as a function of neutron star mass, M (in M_{Sun}), for equations of state with varying empirical parameters (a) energy at saturation, E_{sat}, (b) compressibility, K_{sat}, (c) symmetry energy, J_{sym}, (d) symmetry energy slope, L_{sym}, (e) saturation density, ρ_{sat}, and (f) effective mass, m^*/m. It is obvious from the panels in Figure 4 that the influence of varying the isoscalar parameters, energy per particle at saturation E_{sat} and compressibility K_{sat}, is negligible. Similarly, the variation of the isovector parameters, symmetry energy J_{sym} and its slope L_{sym}, do not vary the f-mode frequencies significantly, as can be seen from the same figure. In Figure 4e, one can see a small non-zero effect of the variation in the saturation density ρ_{sat}. However, the most important influence on the frequencies comes from the variation in the effective nucleon mass m^*/m. In Figure 4f, one can clearly differentiate between the different EoSs with varying effective mass in the f-modes as a function of the stellar mass. The frequencies as a function of NS masses are seen to vary between 2 kHz to 2.6 kHz, and the variation is monotonic with increasing m^*/m. This could have interesting consequences for extracting dense matter physics from the detection of f-mode frequencies for known stellar masses. It is interesting here to compare the above results (obtained within the Cowling approximation and the RMF model framework) with those presented in Ref. [20] (see e.g., the left panel of Figure 3 in Ref. [20]), which were obtained from quite model-independent EoS limits based on low-density nuclear matter and perturbative QCD, using the full linearized oscillation equations.

3.2.2. f-Modes and Tidal Deformability

Among the various NS astrophysical observables that can help to constrain the nuclear EoS, one of the most promising quantities that have recently emerged is tidal deformability. With the discovery of GWs from mergers of NSs, it was seen that, during the inspiral phase, the NSs exert strong gravitational forces on each other, and the deformation produced depends on their EoS [1]. The relation between the dimensionless tidal deformability and the NS compactness, $C = M/R$, is given by $\Lambda = \frac{2k_2}{3C^5}$, where k_2 is the second tidal Love number.
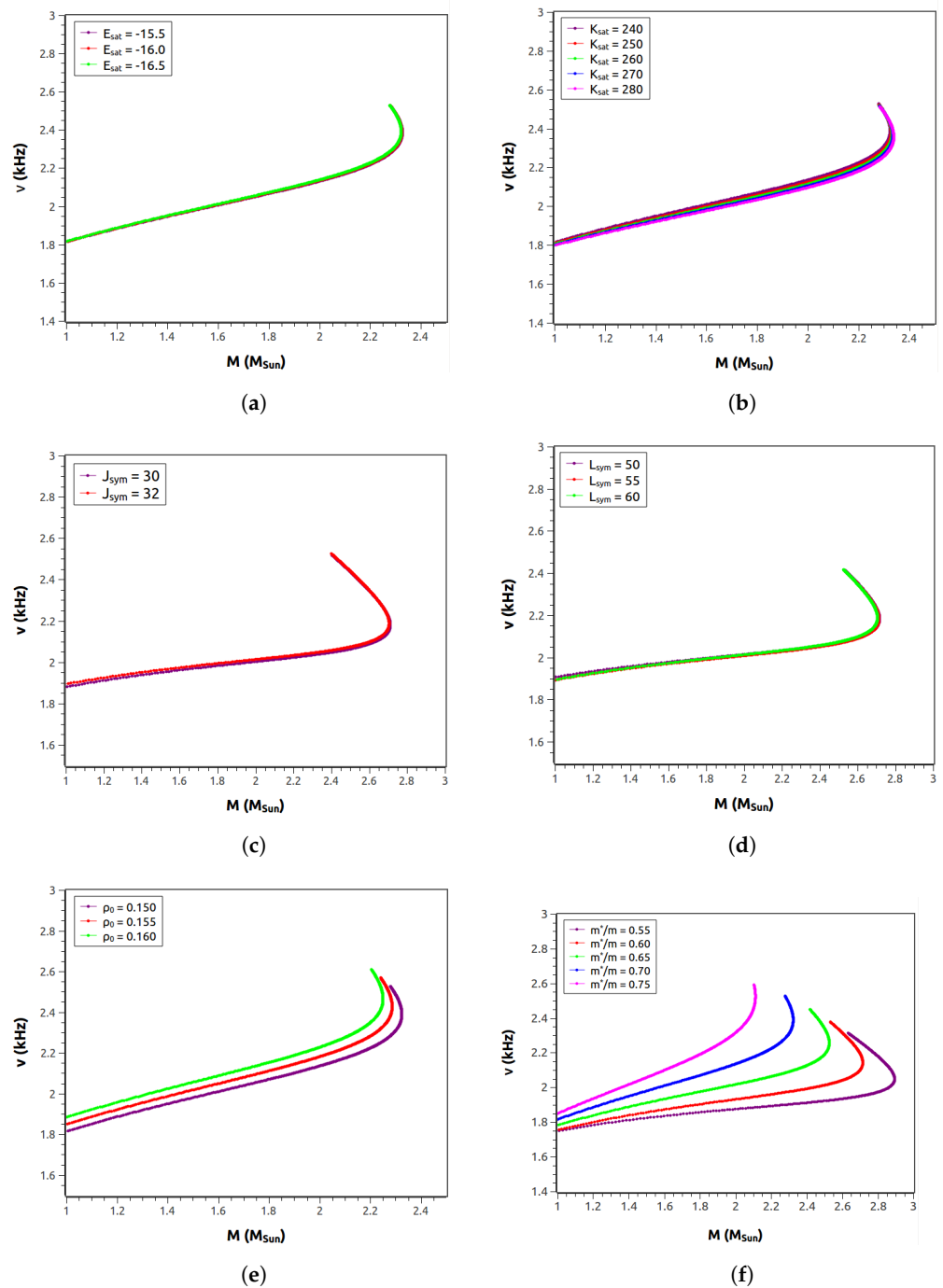
Figure 4. f-mode frequencies, ν, as a function of neutron star mass, M, for equations of state with varying empirical parameters (**a**) energy at saturation E_{sat}, (**b**) compressibility K_{sat}, (**c**) symmetry energy J_{sym}, (**d**) symmetry energy slope L_{sym}, (**e**) saturation density ρ_{sat}, and (**f**) effective mass m^*/m.

In order to estimate the influence of the m^*/m, the dominant empirical parameter that affects the f-mode frequencies, we first demonstrate its effect on the EoS and tidal deformability. In Figure 5, the dimensionless tidal deformability Λ as a function of NS mass is plotted. One can see that the variation of effective nucleon masses m^*/m influences Λ as a function of the NS mass, and the range of values is consistent with recent observations [31,46].
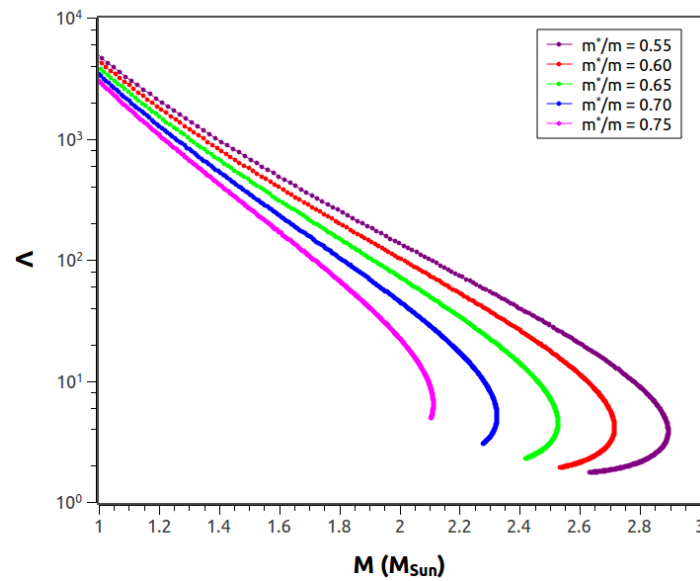
Figure 5. Dimensionless tidal deformability, Λ, as a function of neutron star mass, M, for different effective nucleon masses m^*/m.

Now, consider the influence of variation in m^*/m on the f-mode frequencies ν as a function of Λ, as it is shown in Figure 6. One finds that the variation in effective nucleon masses causes a change in f-mode frequencies in the range (2–2.6) kHz, for a corresponding change in dimensionless tidal deformability in the range $\sim$1–10. From the curves, one can obtain the frequencies corresponding to the lower limit of tidal deformability ($\sim$160, constraints from terrestrial nuclear experiments), and the upper limit of tidal deformability of NSs extracted from the GW170817 event by LIGO and VIRGO Collaborations ($\sim$580) which can provide an interesting constraint for the effective nucleon mass and, hence, the nuclear EoS [17].
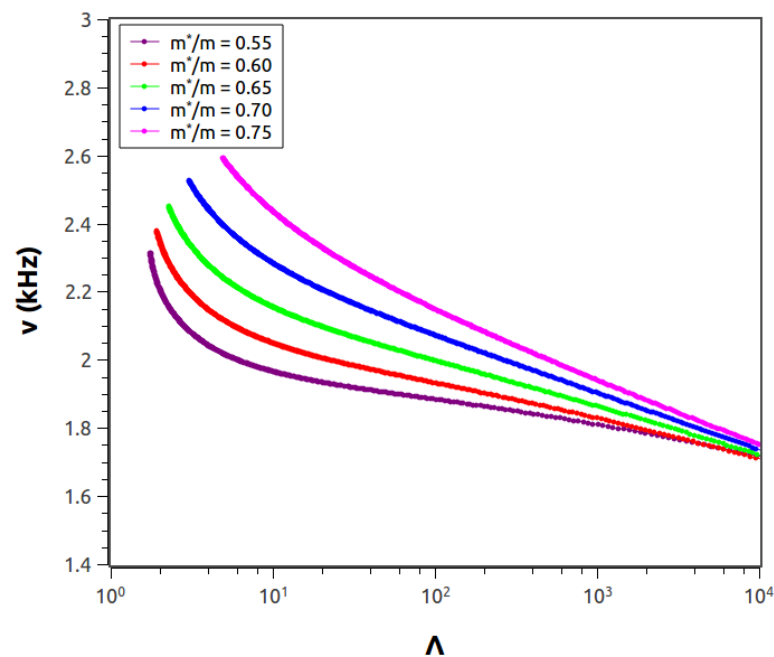

Figure 6. The f-mode frequencies ν as a function of tidal deformability Λ for varying m^*/m.

It was already mentioned in the previous section that tidal deformability is related to stellar compactness. In order to use GW observations to estimate the NS mass and

radius and to differentiate between different families of EoS, empirical relations between the frequency of f-modes and the compactness of the star may be useful [14,15,47]. In Figure 7 the effect of variation of m^*/m on the f-mode frequencies as a function of compactness, $C = M/R$, is shown. Alternatively, one may also derive the compactness from observations of the gravitational redshift Z from spectral lines, as they are related by $Z = (1 - 2C)^{-1/2} - 1$. The corresponding variation of f-mode frequencies as a function of Z is shown in Figure 8.
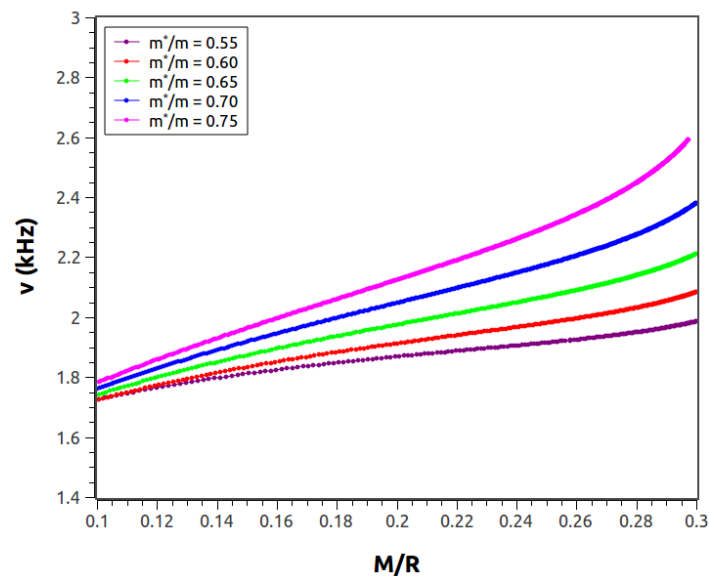
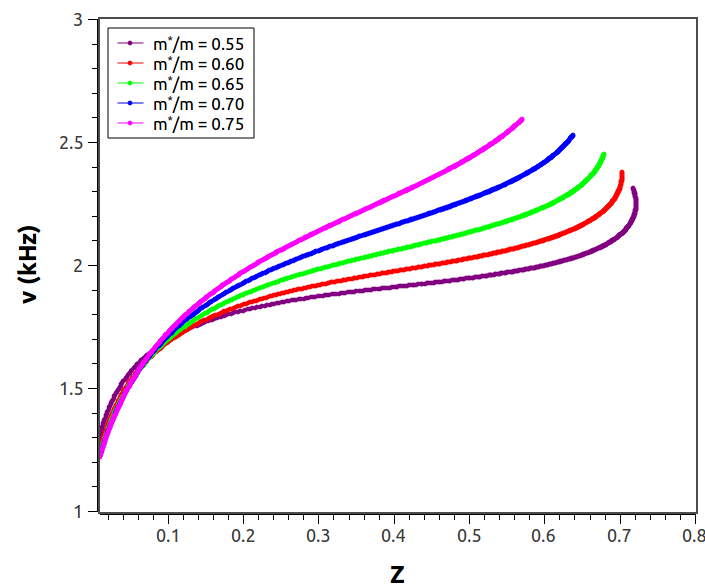**Figure 7.** The f-mode frequencies, ν, as a function of stellar compactness, $C = M/R$, for varying m^*/m.

Figure 8. The f-mode frequencies, ν, as a function of gravitational redshift, Z, for varying m^*/m.

3.3. Asteroseismology Relations for f-Modes

3.3.1. Linear Relation with Average Density

A potentially useful application of the f-mode is that it can be described by universal fitting formulae for asteroseismology, using which the mass and radius of a compact object could be inferred from gravitational wave data. Using polytropic EoSs, it has been shown [14] that the oscillation frequency ν of the fundamental mode has a reasonably

linear dependence on the square root of the average density $(M/R^3)^{1/2}$. This formula was revisited by many authors [15,16,19,47,48] with polytropic or selected phenomenological EoSs, but a comparison of their fits show a dispersion of the results around the fitting curves. Many of the chosen EoSs in those results are no longer consistent with the recent astrophysical observations, such as the maximum mass constraint of M_{Sun}. However, one must distinguish those studies from the analysis in Ref. [20] for a wide range of EoSs, which are consistent with the recent astrophysical data.

In Section 3.2, the dominant nuclear parameters that affect the f-mode frequencies are determined. Now, we will derive the empirical fit relation described above for the entire uncertainty range in the parameter space, namely, in ρ_{sat} and m^*/m. In Figure 9, the $l = 2$ f-mode frequencies as a function of $(M/R^3)^{1/2}$ for varying ρ_{sat} and m^*/m are plotted. A linear fit to the curves, marked by the black dashed line, is obtained, and the equation for the fit is given by:

$$y = 0.857 + 1.435x,$$

where y is the $l = 2$ f-mode frequency as a function of $x = (\bar{M}/\bar{R}^3)^{1/2}$, in terms of the dimensionless variables $\bar{M} = M/(1.4\,M_{Sun})$ and $\bar{R} = R/(10\text{ km})$ [19].

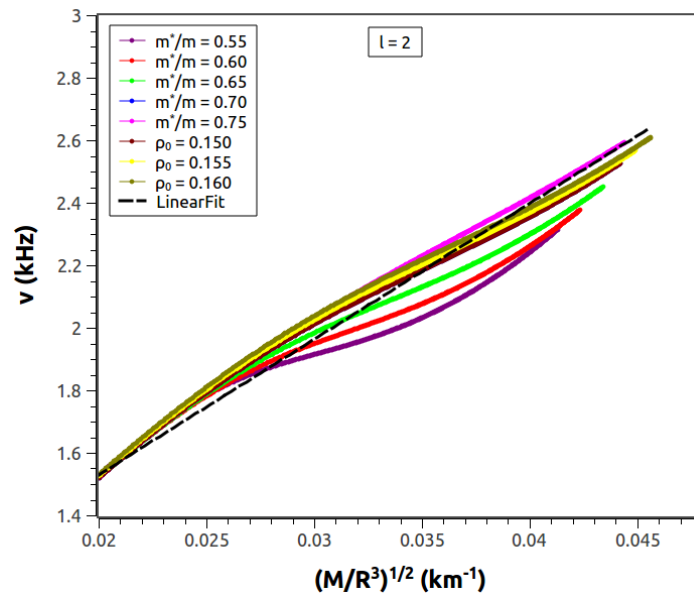**Figure 9.** The $l = 2$ f-mode frequencies as a function of $(M/R^3)^{1/2}$ for varying ρ_{sat} and m^*/m. The black solid line gives the linear fit to the curves.

In comparison with earlier studies [14–16,19,47,48], this is the first time that a sensitivity study to individual nuclear parameters and the effect of their uncertainties on the empirical relations is probed. Here, one must recall the previously calculated [20] f-mode frequencies by solving full perturbation equations for a large range of nuclear EoSs, by considering the maximally soft and stiff EOS compatible with low-density nuclear matter. It is quite useful to compare the results of Figure 9 with the quite model-independent region provided on the left panel of Figure 4 in [20]. In [20], it was pointed out that there is a general spread of the phenomenological EoSs around proposed fit curves in literature, and fairly EoS-independent reliable boundaries were obtained between the fit lines corresponding to hadronic [47] and CFL strange quark matter [42].

3.3.2. Higher-Order f-Modes

In the recent studies [48,49], the instability window relevant to f-modes was investigated and it was concluded that higher-order, e.g., $l = 3, 4$ modes could be more dominant than the quadrupole $l = 2$ mode. Doneva et al. [19] extended the asteroseismology relations for five selected EoSs (of which now three EoSs are ruled out by M_{max} arguments) to $l = 3, 4$

modes. These relations are crucial input for calculating the higher-order mode frequencies in rotating stars. It was also shown that observation of at least of two *f*-modes with different spherical model numbers *l* can be used to determine the mass and radius to a good accuracy, which can be further improved by performing the scheme in an iterative procedure.

With this motivation, a study of the variation of the *f*-mode frequencies as a function of $(M/R^3)^{1/2}$ for higher-order modes $l = 3, 4$ in analogy with $l = 2$ case is performed here. This is given in Figures 10 and 11. The linear fit,

$$y = 1.018 + 1.859x$$

to the curves for the $l = 3$ case is obtained with *y* being the $l = 3$ *f*-mode frequency. Similarly, for the $l = 4$ case, the linear fit is given by:

$$y = 1.156 + 2.215x.$$

With these results, we propose a correction to the fit relations in [19] for the non-rotating limit, by considering the entire uncertainty range of parameter space of saturation nuclear data.
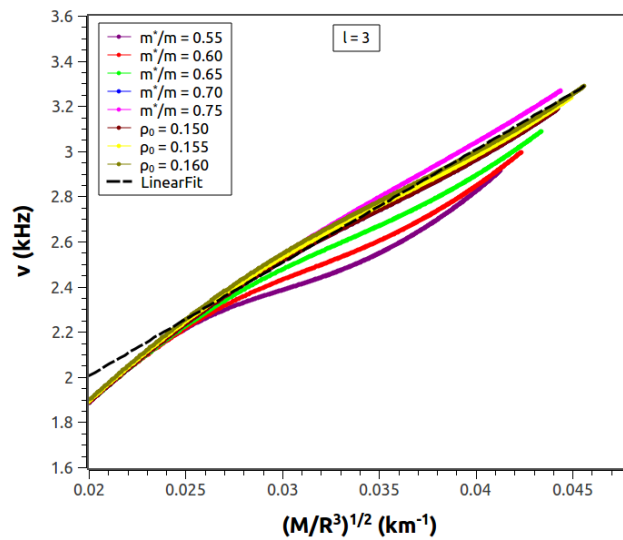

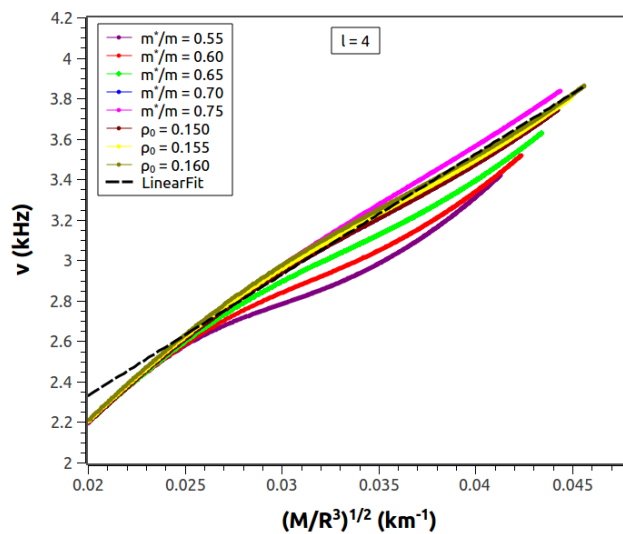**Figure 10.** Same as Figure 9 but for higher-order $l = 3$ mode.

Figure 11. Same as Figure 9 but for higher-order $l = 4$ mode.

3.3.3. Scaled Universal Relations

In Section 3.2.2, the influence of uncertainties of nuclear saturation parameters on empirical relations between the f-mode frequency and stellar parameters such as density and compactness was studied. Here, certain universal relations between the scaled f-mode frequency versus compactness of NSs [15] are investigated. Correlations of the quasi-normal mode frequency appropriately scaled by stellar mass (or radius) with compactness were suggested in [39] for g-modes. It was shown that these phenomenological relations are quite independent of the matter composition. It was also discussed that, using this empirical formula and observing the mode frequencies from gravitational waves, one could determine the stellar properties with high accuracy. Alternatively, with the observation of the gravitational redshift parameter, which is directly related to the stellar compactness, one could put constraints on the stellar mass. Lau [50] first demonstrated the existence of a near-universal relation involving only $M\omega$ and I/M^3, where I is the moment of inertia, which has an accuracy of order 1%. The above mentioned studies demonstrate that semi-universal correlations relating scaled oscillation mode frequencies with a scaled moment of inertia or compactness have much lower uncertainties than unscaled relations involving compactness. Such relations have been investigated more recently in [17,18] for p- and w-modes.

Let us test these hypotheses for the EoSs considered in the current paper. In Figure 12, the frequency scaled by the NS mass, ωM, and in Figure 13, the frequency scaled by the NS radius ωR, are plotted as a function of compactness, C. One observes that ωM indeed retains a universal behavior with C, while ωR shows slight deviation from universal behavior with variation in effective nucleon mass. It is found that the f-mode frequency can be well expressed as a function of stellar compactness M/R using the fit relation,

$$\omega M = 190.364\left(\frac{M}{R}\right) - 5.095. \tag{10}$$

These investigations confirm that, within the uncertainties of the model considered, indeed the scaled semi-universal relations involving oscillation frequencies as a function of compactness have lower uncertainties than those involving unscaled frequencies and, therefore, have a better potential for applications in asteroseismology.
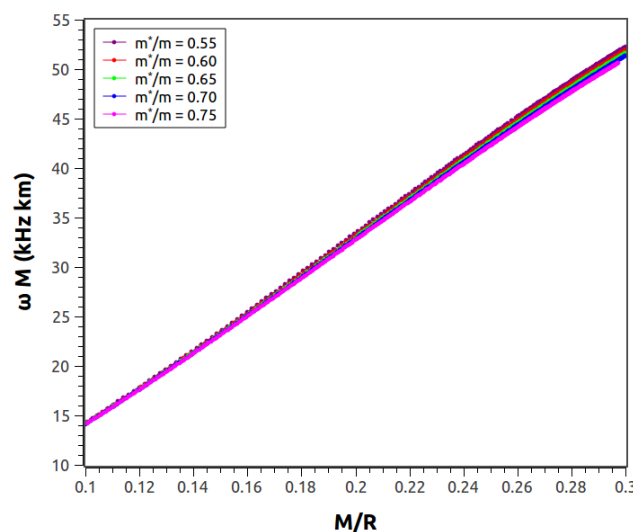

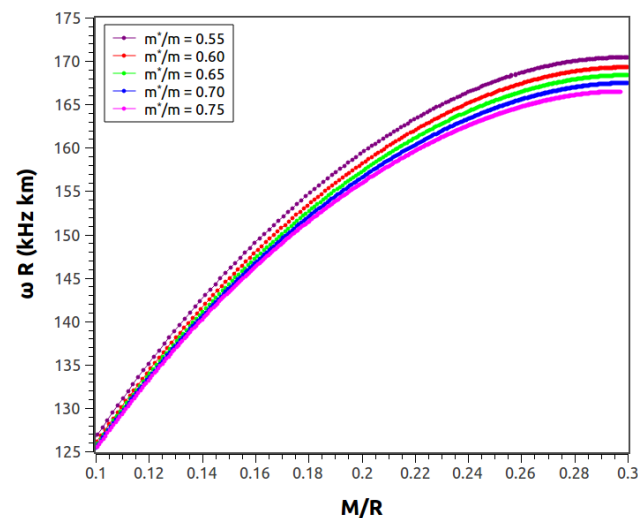**Figure 12.** Scaled f-mode frequency ωM as function of stellar compactness $C = M/R$ for varying m^*/m.

Figure 13. Scaled f-mode frequency ωR (in kHz km) as function of stellar compactness $C = M/R$ for varying m^*/m.

4. Discussions

In this paper, the role of the underlying nuclear physics on f-modes was studied within the Cowling approximation. Within the framework of the relativistic mean field (RMF) model, a systematic investigation of the influence of the uncertainties in empirical nuclear equation of state (EoS) parameters, consistent with recent nuclear experimental data, on the f-mode frequencies was performed. The EoSs, obtained from these parameter sets, all were found to bne compatible with the $2M_{Sun}$ maximum mass limit. It is found that the nucleon in-medium mass to be the most dominant parameter, while the saturation density has a small non-zero effect. Variation in effective mass between 0.55–0.75 resulted in a corresponding variation of f-mode frequencies between (2–2.6) kHz as a function of neutron star (NS) masses.

The effect of uncertainty in effective nucleon mass m^*/m on the relation between f-mode frequencies and tidal deformability, compactness and gravitational redshift was further investigated. These quantities can be derived and to be further constrained with the rapid improvement in multi-messenger astrophysical observations. A future observation of an f-mode frequency from an NS with known mass or tidal deformability would be important for putting a constraint on this EoS parameter.

It was investigated whether the uncertainty in effective mass affects semi-universal asteroseismology relations proposed in literature. Linear fits were ontained for correlations between f-mode frequencies and the square root of the average density, for quadrupole ($l = 2$) and higher-order ($l = 3, 4$) modes. These investigations also confirmed that, within the uncertainties of the model considered, scaled semi-universal relations involving oscillation frequencies as a function of compactness have lower uncertainties than those involving unscaled frequencies. Scaled correlations relating the oscillation frequency with other observables (such as the scaled moment of inertia, tidal deformability) should therefore be probed for potential applications in asteroseismology in future work.

The effective nucleon mass m^*/m results from the interaction of nucleons in the dense medium. Within the RMF model framework, it is shown that it is the dominant parameter that governs f-modes. Several other studies that recently investigated EoS effects in astrophysical scenarios [51–53], using the RMF model as well as other models, also concluded that the nucleon effective mass played a dominant role. To generalize the results obtained here, the role of the effective nucleon mass should also be probed for other microscopic or phenomenological models, along with its density dependence, and this is currently under investigation.

Let us emphasize that the results are obtained here within the Cowling approximation, neglecting background metric perturbations. It is well-known that the use of this

simplification may introduce an uncertainty of the order of 10–30%. Ideally, one must calculate the f-mode frequencies and damping times by solving full perturbation equations. However, the main aim of the present study was to probe the role played by individual nuclear saturation parameters on fundamental f-modes in neutron stars. The result obtained clearly demonstrates that it is the nucleon effective mass that plays a dominant role. Although the application of Cowling approximation limits a direct application of these results to gravitational wave (GW) data, the study in this paper to be considered a first step towards investigation of the role played by different nuclear saturation parameters on f-modes and lays the foundation for an extension to a full calculation including calculation of damping times, with an informed choice of the EoS parameter space resulting from this work. That is currently a work in progress and the results to be communicated in future publications.

In order to extract information about f-modes in NS merger remnants, one must include rotation effects, which were not considered in this paper. In addition, the influence of exotic constituents of matter (hyperons, kaons, deconfined quark matter) on f-modes to be considered [20,41,44].

With the recent detection of GWs from binary compact objects, particularly, mergers of binary neutron stars, prospects of constraining nuclear physics using GWs have become attractive. It has been speculated that f-modes are among the most significant sources of GWs due to the Chandrasekhar–Friedman–Schutz mechanism for isolated NSs and/or in the post-merger scenario. Recent studies suggest that GWs produced by unstable $l = m = 2$ and the $l = m = 4$ f-modes could be detectable by the future Einstein Telescope for sources in the Virgo cluster or for $l = m = 3$ modes even by the LIGO/VIRGO [49]. Then, a possibility of distinguishing between NS EoSs using information about f-modes and NS global observables proves to be very interesting.

References

1. Abbott, B.P.; Abbott, R.; Abbott, T.; Acernese, F.; Ackley, K.; Adams, C.; Adams, T.; Addesso, P.; Adhikari, R.; Adya, V.; et al. GW170817: Observation of gravitational waves from a binary neutron star inspiral. *Phys. Rev. Lett.* **2017**, *119*, 161101. [CrossRef]
2. Abbott, B.P.; Abbott, R.; Abbott, T.; Acernese, F.; Ackley, K.; Adams, C.; Adams, T.; Addesso, P.; Adhikari, R.; Adya, V.; et al. Multi-messenger observations of a binary neutron star merger. *Astrophys. J. Lett.* **2017**, *848*, L12. [CrossRef]
3. Oertel, M.; Hempel, M.; Klähn, T.; Typel, S. Equations of state for supernovae and compact stars. *Rev. Mod. Phys.* **2017**, *89*, 015007. [CrossRef]
4. Demorest, P.B.; Pennucci, T.; Ransom, S.M.; Roberts, M.S.E.; Hessels, J.W.T. A Two-solar-mass neutron star measured using Shapiro delay. *Nature* **2010**, *467*, 1081. [CrossRef]
5. Antoniadis, J.; Freire, P.C.C.; Wex, N.; Tauris, T.M.; Lynch, R.S.; van Kerkwijk, M.H.; Kramer, M.; Bassa, C.; Dhillon, V.S.; Dreibe, T.; et al. A Massive pulsar in a compact relativistic binary. *Science* **2013**, *340*, 448. [CrossRef] [PubMed]
6. Miller, M.C.; Lamb, F.K.; Dittmann, A.J.; Bogdanov, S.; Arzoumanian, Z.; Gendreau, K.C.; Guillot, S.; Harding, A.K.; Ho, W.C.G.; Lattimer, J.M.; et al. PSR J0030+0451 Mass and radius from NICER data and implications for the properties of neutron star matter. *Astrophys. J. Lett.* **2019**, *887*, L24. [CrossRef]
7. Arzoumanian, Z.; Gendreau, K.C.; Baker, C.L.; Cazeau, T.; Hestnes, P.; Kellogg, J.W.; Kenyon, S.J.; Kozon, R.P.; Liu, K.-C.; Manthripragada, S.S.; et al. The Neutron Star Interior Composition Explorer (NICER): Mission definition. *Int. Soc. Opt. Photonics* **2014**, *9144*, 914420.

8. Abbott, B.P.; Abbott, R.; Abbott, T.; Acernese, F.; Ackley, K.; Adams, C.; Adams, T.; Addesso, P.; Adhikari, R.; Adya, V.; et al. GW170817: Measurements of neutron star radii and equation of state. *Phys. Rev. Lett.* **2018**, *121*, 161101. [CrossRef]

9. Abbott, B.P.; Abbott, R.; Abbott, T.; Acernese, F.; Ackley, K.; Adams, C.; Adams, T.; Addesso, P.; Adhikari, R.; Adya, V.; et al. Constraining the *p*-mode-*g*-mode tidal instability with GW170817. *Phys. Rev. Lett.* **2019**, *122*, 061104. [CrossRef]

10. Bauswein, A.; Stergioulas, N.; Janka, H.-T. Exploring properties of high-density matter through remnants of neutron-star mergers. *Eur. Phys. J. A* **2016**, *52*, 56. [CrossRef]

11. Faber, J.A.; Rasio, F.A. Binary neutron star mergers. *Living Rev. Rel.* **2012**, *15*, 8. [CrossRef] [PubMed]

12. Rezzolla, L.; Zanotti, O. *Relativistic Hydrodynamics*; Oxford University Press: Oxford, UK, 2013.

13. Glampedakis, K.; Gualtieri, L. Gravitational waves from single neutron stars: An advanced detector era survey. *Astrophys. Space Sci. Libr.* **2018**, *457*, 673.

14. Andersson, N.; Kokkotas, K.D. Gravitational waves and pulsating stars: What can we learn from future observations? *Phys. Rev. Lett.* **1996**, *77*, 4134. [CrossRef] [PubMed]

15. Andersson, N.; Kokkotas, K.D. Towards gravitational-wave asteroseismology. *Mon. Not. R. Astron. Soc.* **1998**, *299*, 1059. [CrossRef]

16. Schutz, B.F. Asteroseismology of neutron stars and black holes. *J. Phys. Conf. Ser.* **2008**, *118*, 012005. [CrossRef]

17. Wen, D.-H.; Li, B.-A.; Chen, H.-Y.; Zhang, N.-B. GW170817 implications on the frequency and damping time of *f*-mode oscillations of neutron stars. *Phys. Rev. C* **2019**, *99*, 045806. [CrossRef]

18. Blázquez-Salcedo, J.L.; González-Romero, L.M.; Navarro-Lérida, F. Polar quasi-normal modes of neutron stars with equations of state satisfying the $2M_\odot$ constraint. *Phys. Rev. D* **2014**, *89*, 044006. [CrossRef]

19. Doneva, D.D.; Gaertig, E.; Kokkotas, K.D.; Krüger, C. Gravitational wave asteroseismology of fast rotating neutron stars with realistic equations of state. *Phys. Rev. D* **2013**, *88*, 044052. [CrossRef]

20. Flores, C.V.; Lugones, G. Gravitational wave asteroseismology limits from low density nuclear matter and perturbative QCD. *J. Cosmol. Astropart. Phys.* **2018**, *8*, 46. [CrossRef]

21. Horowitz, C.J.; Serot, B.D. Self-consistent hartree description of finite nuclei in a relativistic quantum field theory. *Nucl. Phys. A* **1981**, *368*, 503. [CrossRef]

22. Horowitz, C.J.; Piekarewicz, J. Neutron star structure and the neutron radius of ^{208}Pb. *Phys. Rev. Lett.* **2001**, *86*, 5647. [CrossRef]

23. Fattoyev, F.J.; Piekarewicz, J. Relativistic models of the neutron-star matter equation of state. *Phys. Rev. C* **2010**, *82*, 025805. [CrossRef]

24. Chen, W.-C.; Piekarewicz, J. Building relativistic mean field models for finite nuclei and neutron stars. *Phys. Rev. C* **2014**, *90*, 044305. [CrossRef]

25. Hornick, N.; Tolos, L.; Zacchi, A.; Christian, J.-E.; Schaffner-Bielich, J. Relativistic parameterizations of neutron matter and implications for neutron stars. *Phys. Rev. C* **2018**, *98*, 065804. [CrossRef]

26. Glendenning, N.K.; Moszkowski, S.A. Reconciliation of neutron-star masses and binding of the Λ in hypernuclei. *Phys. Rev. Lett.* **1991**, *67*, 2414. [CrossRef]

27. Glendenning, N.K. *Compact Stars*; Springer: New York, NY, USA, 2000.

28. Yagi, K.; Yunes, N. I-Love-Q relations in neutron stars and their applications to astrophysics, gravitational waves, and fundamental physics. *Phys. Rev. D* **2013**, *88*, 023009. [CrossRef]

29. Annala, E.; Gorda, T.; Kurkela, A.; Vuorinen, A. Gravitational-wave constraints on the neutron-star-matter equation of state. *Phys. Rev. Lett.* **2018**, *120*, 172703. [CrossRef] [PubMed]

30. Most, E.R.; Weih, L.R.; Rezzolla, L.; Schaffner-Bielich, J. New constraints on radii and tidal deformabilities of neutron stars from GW170817. *Phys. Rev. Lett.* **2018**, *120*, 261103. [CrossRef]

31. De, S.; Finstad, D.; Lattimer, J.M.; Brown, D.A.; Berger, E.; Biwer, C.M. Tidal deformabilities and radii of neutron stars from the observation of GW170817. *Phys. Rev. Lett.* **2018**, *121*, 091102. [CrossRef]

32. Thorne, K.S.; Campolattaro, A. Non-radial pulsation of general-relativistic stellar models. I. Analytic analysis for L >= 2. *Astrophys. J.* **1967**, *149*, 591. [CrossRef]

33. Kokkotas, K.D.; Schmidt, B.G. Quasi-normal modes of stars and black holes. *Living Rev. Relativ.* **1999**, *2*, 1. [CrossRef]

34. Chandrasekhar, S.; Ferrari, V. On the non-radial oscillations of a star. *Proc. Roy. Soc. Lond. A* **1991**, *432*, 247.

35. Detweiler, S.; Lindblom, L. On the nonradial pulsations of general relativistic stellar models. *Astrophys. J.* **1985**, *292*, 12. [CrossRef]

36. Thorne, K.S. Nonradial pulsation of general-relativistic stellar models. III. Analytic and numerical results for neutron stars. *Astrophys. J.* **1969**, *158*, 1. [CrossRef]

37. Thorne, K.S. Nonradial pulsation of general-relativistic stellar models. IV. The weakfield limit. *Astrophys. J.* **1969**, *158*, 997. [CrossRef]

38. Thorne, K.S. Gravitational radiation damping. *Phys. Rev. Lett.* **1968**, *21*, 320. [CrossRef]

39. Sotani, H.; Yasutake, N.; Maruyama, T.; Tatsumi, T. Signatures of hadron-quark mixed phase in gravitational waves. *Phys. Rev. D* **2011**, *83*, 024014. [CrossRef]

40. Cowling, T.G. The Non-radial oscillations of polytropic stars. *Mon. Not. R. Astron. Soc* **1941**, *101*, 367 . [CrossRef]

41. Flores, C.V.; Lugones, G. Discriminating hadronic and quark stars through gravitational waves of fluid pulsation modes. *Class. Quantum Grav.* **2014**, *31*, 155002. [CrossRef]

42. Flores, C.V.; Lugones, G. Constraining color flavor locked strange stars in the gravitational wave era. *Phys. Rev. C* **2017** *95*, 025808. [CrossRef]

43. Tonetto, L.; Lugones, G. Discontinuity gravity modes in hybrid stars: Assessing the role of rapid and slow phase conversions. *Phys. Rev. D* **2020**, *101*, 123029. [CrossRef]

44. Ranea-Sandoval, I.F.; Guilera, O.M.; Mariani, M.; Orsaria, M.G. Oscillation modes of hybrid stars within the relativistic Cowling approximation. *J Cosmol. Astropart. Phys.* **2018**, *12*, 31. [CrossRef]

45. Sotani, H. Gravitational wave asteroseismology for low-mass neutron stars. *Phys. Rev. D* **2020**, *102*, 063023. [CrossRef]

46. Abbott, B.P.; Abbott, R.; Abbott, T.; Acernese, F.; Ackley, K.; Adams, C.; Adams, T.; Addesso, P.; Adhikari, R.; Adya, V.; et al. Model comparison from LIGO–Virgo data on GW170817's binary components and consequences for the merger remnant. *Class. Quantum Grav.* **2020**, *37*, 045006. [CrossRef]

47. Benhar, O.; Ferrari, V.; Gualtieri, L. Gravitational waves from neutron stars described by modern EOS. *AIP Conf. Proc.* **2005**, *751*, 211.

48. Gaertig, E.; Glampedakis, K.; Kokkotas, K.D.; Zink, B. f-Mode instability in relativistic neutron Stars. *Phys. Rev. Lett.* **2011**, *107*, 101102. [CrossRef]

49. Passamonti, A.; Gaertig, E.; Kokkotas, K.D.; Doneva, D. Evolution of the f-mode instability in neutron stars and gravitational wave detectability. *Phys. Rev. D* **2013**, *87*, 084010. [CrossRef]

50. Lau, H.K.; Leung, P.T.; Lin, L.M. Inferring physical parameters of compact stars from their f-mode gravitational wave signals. *Astrophys. J.* **2010**, *714*, 1234. [CrossRef]

51. Alvarez-Castillo, D.E.; Ayriyan, A.; Barnaföldi, G.G.; Grigorian, H.; Pósfay, P. Studying the parameters of the extended $\sigma - \omega$ model for neutron star matter. *Eur. Phys. Spec. Top.* **2020**, *229*, 3615. [CrossRef]

52. Alvarez-Castillo, D.E.; Ayriyan, A.; Barnaföldi, G.G.; Pósfay, P. Estimating the values and variations of Neutron Star observables by dense nuclear matter properties. *Phys. Part. Nucl.* **2020**, *51*, 725. [CrossRef]

53. Schneider, A.S.; Roberts, L.F.; Ott, C.D.; O'Connor, E. Equation of state effects in the core collapse of a 20-$M_\odot$ star. *Phys. Rev. C* **2019**, *100*, 055802. [CrossRef]